

Spectroscopic capabilities of the time-resolved magnetic field effect technique as illustrated in the study of hexamethylethane radical cation in liquid hexane

Victor A. Bagryansky,^{*ab} Vsevolod I. Borovkov^{ab} and Yuri N. Molin^{ab}

^a Institute of Chemical Kinetics and Combustion, Siberian Branch of Russian Academy of Sciences, 630090, Novosibirsk, Russia. E-mail: vbag@ns.kinetics.nsc.ru; Fax: +7 3832 342350; Tel: +7 3832 331561

^b Novosibirsk State University, 630090, Novosibirsk, Russia

Received 16th September 2003, Accepted 7th January 2004
First published as an Advance Article on the web 3rd February 2004

The method of the time-resolved magnetic field effect in the recombination fluorescence of spin-correlated radical ion pairs can provide information on the parameters of the EPR spectra of short-lived radical ions. The present paper demonstrates these spectroscopic potentialities using, as an example, hexamethylethane radical cation whose EPR spectrum in solution is determined by isotropic hfc with 18 equivalent protons. The hfc constant is determined from the position of peaks of the time-resolved magnetic field effect of the hexamethylethane and perdeuterated *p*-terphenyl solution in *n*-hexane at ambient temperature. The difference in the *g*-values of (hexamethylethane)^{•+} and (*p*-terphenyl-*d*₁₄)^{•-} radical ions is found by analyzing the curve shape of magnetic field effect for various magnetic field strength. Both the hfc constant and the difference in the *g*-values coincide with the data obtained by the OD EPR method. Independence of the curve shape on hexamethylethane concentration testifies to the low rate of ion-molecular charge transfer. The method of time resolved magnetic field effect is used to determine the times of longitudinal and transverse paramagnetic relaxation. The dependency of the relaxation rates on magnetic field strength is derived and feasible relaxation mechanisms are discussed.

Introduction

Organic radical ions are intermediates in the reactions of many types especially in radiation-chemical processes. At temperatures close to room temperature the lifetimes of these particles are, as a rule, as short as 1–100 nanoseconds. Therefore, the properties of radical ions were studied by either their stabilization in low-temperature matrices¹ or the time-resolved methods such as transient optical absorption,² microwave³ or direct current⁴ conductivity, *etc.* Each method has its own advantages and limitations. Experiments in matrices allow one in many cases to reach the concentration of radical ions sufficient for them to be recorded by the EPR method, but fail to give any information on the rates of radical ion reactions in solutions at usual temperatures. The methods of transient absorption and current conductivity are of limited usefulness in radical identification.

The method of optically detected EPR (OD EPR) in stationary⁵ and time-resolved⁶ variants was successfully applied for recording the EPR spectra of radical ions involved in spin-correlated pairs in solutions. Since this method displays a higher sensitivity as compared with the conventional EPR method, it was first used to record the EPR spectra of a series of radical ions at room temperature.^{5,6} However, the method has a substantial disadvantage as applied to radical ions with very short lifetimes. The OD EPR signal intensity is the higher the larger is the rotation angle of the electron spin under the action of the resonance mw field in the radical lifetime. Therefore it is necessary to use a high-level mw field power. Thus, to attain a 90° spin rotation during 10 ns, the mw field amplitude should be 0.9 mT. The use of high mw fields leads to the broadening of spectrum lines and, thus, to a partial loss of spectral information.

Another method giving information on the EPR spectra of short-lived radical ions is the method of time-resolved magnetic field effect (TR MFE) in recombination fluorescence.^{7–11} This method can be used to register radical ions with lifetimes up to several nanoseconds. As shown earlier, the method can be employed to determine the hfc constants of radical ions with equivalent nuclei,⁹ the second moment of unresolved EPR spectrum,^{10,11} and the difference in the *g*-factors of paired radical ions in the case of unresolved spectra.¹¹ In the present paper, we discuss the potentialities of this method using experiments recording the hexamethylethane radical cation as an example. This radical exhibits a resolved EPR spectrum with the known constants and *g*-factors and thus is a convenient object for revealing the spectroscopic capabilities of the TR MFE method including the determination of the times of paramagnetic relaxation.

The TR MFE method: Basic theoretical formulas

In the TR MFE experiment, a short pulse of ionizing radiation in a solution of electron and hole acceptors, gives rise to radical ion pairs in the singlet correlated spin state. Luminophore with a high quantum yield and short fluorescence time is used as one of the charge acceptors. By the time of recombination, the pair singlet state can convert into the triplet one due to hyperfine interaction, the difference in the *g*-factors of pair radicals and paramagnetic relaxation. The experimentally measured value is the fluorescence intensity *I*(*t*) of pairs recombination product in the singlet spin state. The intensity for a fairly short luminophore fluorescence time, obeys the equation

$$I(t) \propto F(t) \left[\theta \rho_{SS}(t) + \frac{1}{4}(1 - \theta) \right] \quad (1)$$

where $F(t)$ is the rate of radical ion pairs recombination, θ is the fraction of the pairs originating in the spin-correlated singlet state, and $\rho_{SS}(t)$ is the population of the singlet state of these pairs at time t . It is assumed that the remaining fraction $(1 - \theta)$ of pairs is in the fully noncorrelated state.

It is known¹² that the time evolution of singlet population contains complete information on the EPR spectrum of a radical pair. Thus, if spin evolution occurs in the high magnetic field, the singlet population, as a time function, is related to the EPR spectrum *via* the Fourier transform. Unfortunately, the problem of extracting the EPR spectrum directly from fluorescence kinetics $I(t)$ is complicated by its dependence on the $F(t)$ function that depends on the mutual spatial distribution of pair radicals and cannot be described in terms of analytical functions. This difficulty can be minimized using the ratio of the fluorescence kinetics measured in the external magnetic field to the kinetics without field

$$\frac{I_H(t)}{I_0(t)} = \frac{\theta \rho_{SS}^H(t) + \frac{1}{4}(1 - \theta)}{\theta \rho_{SS}^0(t) + \frac{1}{4}(1 - \theta)} \quad (2)$$

called the time-resolved magnetic field effect (TR MFE).

EPR spectrum parameters can be determined from the TR MFE curve by calculating eqn. (2) with the parameters values giving the best fit to the experiment. There is no analytical expression for singlet population in the general case. One of the simplest cases allowing analytical solution is that of isotropic hfc with equivalent nuclei in one of the radical ions and small unresolved hfc in the other.¹²⁻¹⁴ In the following expressions describing the singlet population for this case, the indices a and b denote the values referring to these two radicals, respectively,

$$\rho_{SS}^H(t) = \frac{1}{4} + \frac{1}{4} e^{-t/T_1} \langle f(t) \rangle + \frac{1}{2} e^{-t/T_2} e^{\sigma_b^2 t^2 / 2} \text{Re}(\langle h(t) \rangle e^{-i\omega_b t}) \quad (3)$$

Here

$$f(t) = 1 - \frac{a^2}{2I+1} \sum_{m=-I}^I \frac{I(I+1) - m(m+1)}{(2R_m)^2} [1 - \cos(2R_m t)],$$

$$h(t) = \frac{1}{4(2I+1)} \sum_{m=-I}^I [(1 + D_m) e^{iR_m t} + (1 - D_m) e^{-iR_m t}] \times [(1 + D_{m-1}) e^{iR_{m-1} t} + (1 - D_{m-1}) e^{-iR_{m-1} t}]$$

$$2R_m = \sqrt{\omega_a^2 + a\omega_a(2m+1) + a^2 \left(I + \frac{1}{2}\right)^2},$$

$$D_m = \frac{\omega_a + a(m+1/2)}{2R_m}, \quad \omega_{a,b} = \frac{g_{a,b} \beta B}{\hbar},$$

B is the magnetic field strength, g is the radical g -value, a is a hfc constant in the first radical (in units of circular frequency), σ_b^2 is the second moment of the EPR spectrum of the second radical.

For high magnetic field paramagnetic relaxation is taken into account in the simplest model of the longitudinal and transverse paramagnetic relaxation times T_1 and T_2 relating to transition with and without electron spin flip, respectively. For weak field these times are assumed to be equal. A more rigorous consideration of relaxation requires more details about its mechanism.

The angular brackets in eqn. (3) denote averaging over the values of the total nucleus spin I . When there are n equivalent nuclei with spin $\frac{1}{2}$, the coefficients of this distribution are of the form

$$P_I = \frac{(2I+1)^2 n!}{2^n (n/2 - I)(n/2 + I + 1)} \quad (4)$$

For the cases of high field $\omega \gg a$, and zero field, $\omega = 0$, the equations for the singlet state population becomes much simpler

$$\rho_{SS}^H(t) = \frac{1}{4} + \frac{1}{4} e^{-t/T_1} + \frac{1}{2} e^{-t/T_2} e^{-\sigma_b^2 t^2 / 2} \times \cos \frac{(g_a - g_b) \beta B t}{\hbar} \left(\cos \frac{at}{2} \right)^n \quad (5)$$

$$\rho_{SS}^0(t) = \frac{1}{4} + \frac{1}{12} e^{-t/T_0} \left[1 + 2(1 - \sigma_b^2 t^2) e^{\sigma_b^2 t^2 / 2} \right] \times \left[\frac{n+3}{n+1} + \frac{2n(n+2)}{n+1} \left(\cos \frac{at}{2} \right)^{n+1} - 2n \left(\cos \frac{at}{2} \right)^{n-1} \right] \quad (6)$$

In this case, T_0 is the time of phase relaxation in zero field.

Fig. 1 shows the results of the modeling of magnetic field effect (2) calculated from eqns. (3)–(4) for the various values of the magnetic field strength. In the calculation, it is assumed that $\sigma_b = 0$, $T_1 = T_2 = \infty$, $(g_a - g_b) = 0.001$, and $\theta = 0.2$. In field with the strength exceeding 20 times the hfc constant, the calculation gives the known pattern for periodic alternation of the peaks for which the position of the first peak is determined by the second spectrum moment, and that of the second peak is determined by the hfc constant.⁹ We proved by calculations that for $n > 2$ the ratio of first and second peaks times is approximately equal to $2n^{1/2}$. The field with strength of $2a$ comparable with hfc constant the curve exhibits additional frequencies that complicate the pattern of beats. In the fields with high strengths (500 a and 1000 a), the influence of the difference in radical g -factors is noticeable, which is manifested in a periodic 'partial reversing' of the mentioned above peculiarities. This is due to a cosine in the last term of eqn. (5) with an argument depending on the difference in radical g -value. Taking into account the relaxation leads to the peaks being damped and the rise and fall of the basic line in which the beat peaks are situated. Thus, the main spectral parameters such as hfc constant, the number of magnetic nuclei, and the difference in radical g -factors can be determined from the shape of the magnetic field effect curve and its dependence on magnetic field strength.

Experimental

The decay of the delayed fluorescence of the n -hexane solutions of hexamethylethane (HME) and p -terphenyl- d_{14}

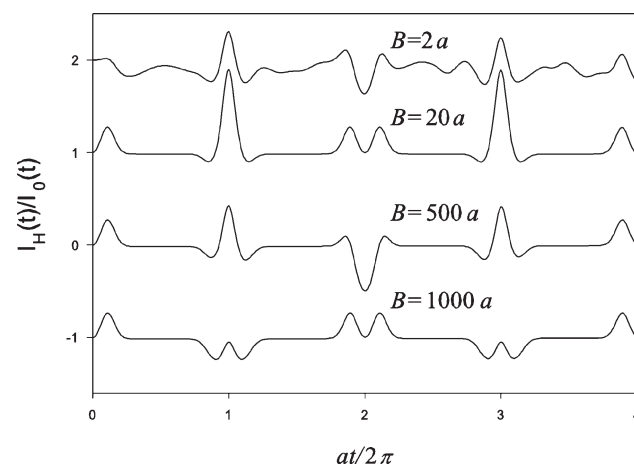


Fig. 1 The calculated TR MFE curves obtained from eqns. (2)–(4) in various magnetic fields for a radical pair in which one of the partners has no hfc and the second one has 18 equivalent protons with hfc constant a . The difference in g -factors is assumed to be $\Delta g = 0.001$, the fraction of spin-correlated pairs $\theta = 0.2$. Paramagnetic relaxation is neglected. For convenience, the curves are arbitrarily shifted along the vertical.

(pTP- d_{14}) was detected by the single photon counting technique using an X-ray fluorimeter described elsewhere.¹⁵ The duration of the ionizing pulse was <3 ns. The light was collected using an optical pass band filter (260–390 nm). The sample cuvette was similar to that described elsewhere.¹⁶ It was constructed to avoid the irradiation of the quartz parts of the cuvette and to minimize the background luminescence.

To decrease the influence of instrumental drift the fluorescence decays were registered for periods of 250 s, alternatively, with and without magnetic field using computer control. Zero magnetic field was adjusted to within ± 0.05 mT. The thermostabilization system allowed us to keep the sample temperature in the range from -20 to $+50$ °C with an accuracy of ± 1 °C.

The OD EPR spectrometer has been described in detail elsewhere.¹⁷ About 1 ml of a sample solution in a quartz cuvette was put in the magnetic field of a BRUKER ER-200D EPR spectrometer equipped with an X-ray tube (Mo, 45 kV, 50 mA) for sample irradiation and a photomultiplier tube with a quartz light guide for the registration of recombination fluorescence. The spectrometer was supplied with a home made mw amplifier for raising power level up to 10 W. *n*-Hexane (Reactiv, Russia) was stirred with concentrated sulfuric acid, washed with water, distilled over sodium and passed through a 1 m column of activated alumina and then passed through a 1 m column of activated alumina coated by AgNO_3 (Reactiv, Russia). HME (Aldrich) and pTP- d_{14} (Aldrich) was used as received. The solutions were degassed by repeated freeze-pump-thaw cycles.

Results and discussion

Our attempts to record the OD EPR spectrum of the $(\text{HME})^{+\cdot}$ radical cation in *n*-hexane at room temperature have failed, probably, because the recombination time of pairs in a nonviscous *n*-hexane was too short to provide a substantial change in singlet population under the action of mw field. It is known, however, that at low temperatures the OD EPR spectrum of this radical cation can be recorded.^{18,19} Therefore we performed the experiment in *n*-hexane at lower temperature.

Fig. 2 shows the OD EPR spectrum of the 0.1 M HME + 3×10^{-4} M pTP- d_{14} solution in *n*-hexane at 268 K. Due to the ionization energy difference (9.8 eV for HME and 10.13 eV for *n*-hexane²⁰), the holes resulting from *n*-hexane ionization are captured mainly by the HME molecules. The electrons are captured by the pTP- d_{14} ones. Thus, the OD EPR signal is expected to arise from the recombination of $(\text{HME})^{+\cdot}/(\text{pTP-}d_{14})^{\cdot-}$ pairs, which is accompanied by the fluorescence of pTP- d_{14} molecules. As follows from Fig. 2,

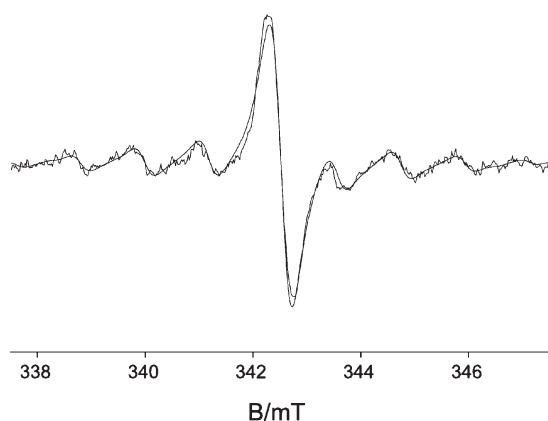


Fig. 2 The OD EPR spectrum of the 0.1 M HME + 3×10^{-4} M pTP- d_{14} solution in *n*-hexane at 268 K. Smooth line is the best approximation of the experiment by the model of the superposition of the $(\text{pTP-}d_{14})^{\cdot-}$ and $(\text{HME})^{+\cdot}$ spectra with the hfc constant $a(18\text{H}) = 1.2$ mT and the difference in the g -factors $\Delta g = 9 \times 10^{-4}$.

the spectrum is the superposition of a singlet and a multiplet with an odd number of lines separated by (1.2 ± 0.05) mT. The multiplet splitting is close to hfc constant $a(18\text{H}) = 1.22$ mT in the HME radical cation produced in *n*-pentane at 190 K and in CFCl_3 at 140 K.¹⁸ In addition, this value is in agreement with the data obtained in a low CFCl_3 matrix at 77 K $a(6\text{H}) = 3.2$ mT and $a(12\text{H}) = 0.45$ mT,²¹ taking into account the fast rotation of methyl groups in our experimental conditions and assuming the same sign of both hfc constants. In Fig. 2, the width of individual lines is 0.5 mT and is determined by the mw field amplitude. The thin smooth line denotes the best approximation of the experiment by the model of the superposition of the $(\text{pTP-}d_{14})^{\cdot-}$ and $(\text{HME})^{+\cdot}$ spectra with the hfc constant $a(18\text{H}) = 1.2$ mT. The integral intensities of the spectra are identical. Their relative shift corresponds to a larger value of the radical cation g -factor by the value $\Delta g = (9 \pm 1) \times 10^{-4}$. Thus, using rather high mw power, the OD EPR method can give the EPR spectrum of $(\text{HME})^{+\cdot}$ radical cation in solution at the temperature close to ambient. However, in this case, it is impossible to measure the individual line width.

Fig. 3 shows the experimental TR MFE curves for the 0.1 M HME + 3×10^{-5} M pTP- d_{14} solution in *n*-hexane in fields of 0.1, 0.5 and 0.7 T. One can see from the Fig. 3 a decaying peaks sequence. As the magnetic field strength increases, the peaks observed at long times reverse, which indicates the difference in the g -factors of the pair radical ions. Smooth lines show the results from the approximation of experiment by eqn. (2), in which the finite time of pTP- d_{14} fluorescence, $\tau = 1.2$ ns,²² was taken into account by convolution the expression for the singlet population with the exponential fluorescence kinetics. The fraction of spin-correlated pairs θ , the relaxation times T_0 , T_1 , and T_2 , the values of Δg and the hfc constant a were used as fitting parameters for better agreement with the experiment. The following optimum values were obtained for these parameters: $a = (1.24 \pm 0.03)$ mT, $\Delta g = (7 \pm 1) \times 10^{-4}$, and $\theta = 0.18 \pm 0.02$. Experiments performed in various fields differ only in the relaxation times T_1 and T_2 , whose values increase with increasing the magnetic field strength (Fig. 6). The values for Δg and hfc constant are close to the data obtained by the OD EPR method.

Usually the paramagnetic relaxation time values T_2 for radical ions, obtained by TR MFE technique, are much lower than

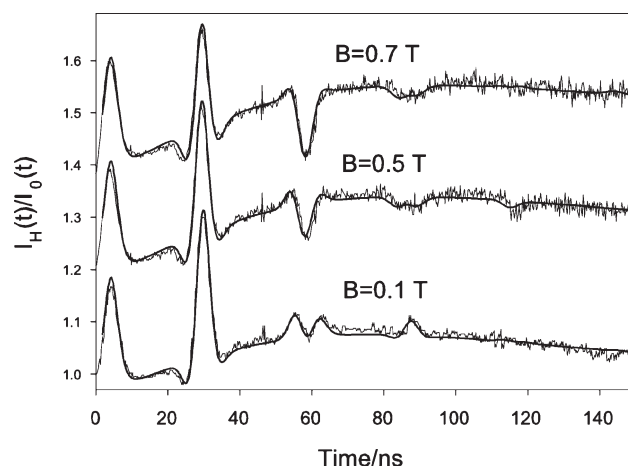


Fig. 3 Experimental TR MFE curves for the 0.1 M HME + 3×10^{-5} M pTP- d_{14} solution in *n*-hexane at 293 K in various magnetic fields. Smooth lines are the approximation of experiment by the model of $(\text{HME})^{+\cdot}/(\text{pTP-}d_{14})^{\cdot-}$ pairs with the parameters: $\sigma(\text{pTP-}d_{14}) = 0.067$ mT, $a(18\text{H}) = 1.24$ mT, $\Delta g = 7 \times 10^{-4}$, $\theta = 0.18$, and $\tau_{\text{fl}} = 1.2$ ns. Relaxation times: for $B = 0.1$ T $T_1 = 114$ ns, $T_2 = 38$ ns; for $B = 0.5$ T $T_1 = 227$ ns, $T_2 = 43$ ns; for $B = 0.7$ T $T_1 = 320$ ns, $T_2 = 50$ ns, for all the curves $T_0 = 46$ ns. For convenience, the curves are arbitrarily shifted along the vertical.

the typical values characterizing the neutral radicals in liquid.^{9–11} A similar peculiarity was also observed in OD EPR technique.⁵ The majority of radical ion pairs in solutions have an individual line width exceeding 0.1 mT. This value corresponds to the phase relaxation times of radical ions that are shorter than 60 ns. To study the relaxation mechanism for the (HME)⁺ radical cation, we measured the concentration and temperature dependences of TR MFE. A change in the HME concentration from 0.1 to 0.5 M failed to cause any changes in the shape of the TR MFE curves. It was concluded then that the contribution of the degenerate electron exchange between a radical cation and a neutral molecule of HME to paramagnetic relaxation was not substantial. There was also no significant temperature dependence of the curve shapes and thus, of the relaxation times over the range of –20 to +50 °C (see Fig. 4).

Fig. 5 shows the experimental data obtained in fields of 2 and 4 mT comparable with the hfc constant. In this case, the TR MFE curves exhibit a more complex shape as compared with the high fields. Nevertheless, these oscillations are well reproduced by simulation using eqns. (2)–(4) (smooth lines in Fig. 5), which allows us to determine the paramagnetic relaxation times T_1 and T_2 that coincide in these fields with the value of the relaxation time T_0 in zero field.

The relaxation time T_1 was found to depend substantially on the magnetic field strength while T_2 is nearly constant. This is shown by Fig. 6 giving the data on all measured fields as the dependences of the rates of longitudinal and transverse relaxation on the magnetic field strength.

According to the Redfield theory,²³ when the amplitude of perturbation that causes relaxation is independent of field strength, both of the rates should decrease with increasing field strength B according to the equations:

$$\frac{1}{T_1} = \frac{2\gamma^2\Delta^2\tau}{1 + (\gamma B\tau)^2} \quad (7)$$

$$\frac{1}{T_2} = \frac{1}{2} \left(\frac{1}{T_1} + 2\gamma^2\Delta^2\tau \right) \quad (8)$$

where γ is the gyromagnetic ratio, Δ and τ are the amplitude and correlation time of the process that causes relaxation.

These equations predict that the rates of T_1 and T_2 relaxation in weak fields should coincide. With increasing field the T_1 relaxation rate should vanish, and the T_2 relaxation rate should drop down to half its value in weak field.

As seen from Fig. 6, the T_1 relaxation rate decreases with magnetic field strength in accordance with the prediction of the theory. The lower solid curve in the figure was calculated

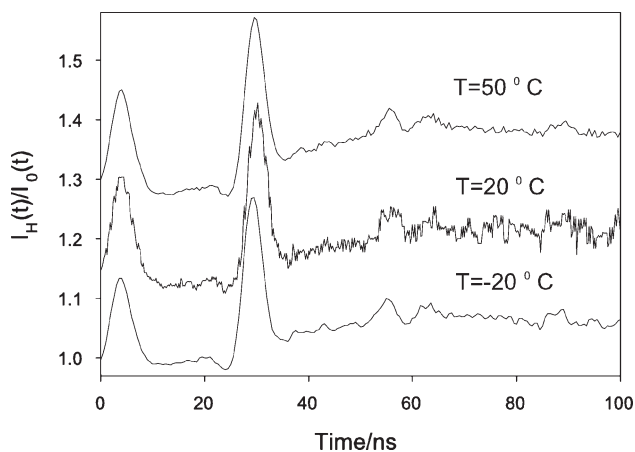


Fig. 4 The TR MFE curves for the 0.3 M HME + 3×10^{-5} M pTP- d_{14} solution in n -hexane at various temperatures. For convenience, the curves are arbitrarily shifted along the vertical.

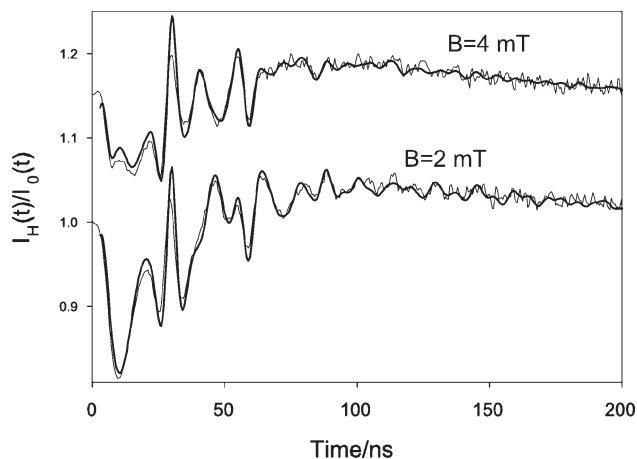


Fig. 5 The TR MFE curves for the 0.3 M HME + 3×10^{-5} M pTP- d_{14} solution in n -hexane in low magnetic fields. Smooth lines are the approximation of experiment by the model of the (HME)⁺/(pTP- d_{14})⁺ pairs with parameters: $a(18H) = 1.24$ mT, $\theta = 0.18$, $\tau_H = 1.2$ ns, $T_1 = T_2 = T_0 = 46$ ns. For convenience, the curve for 4 mT is shifted along the vertical.

using eqn. (7) with best fit parameters $\tau = 10$ ps and $\Delta = 3.1$ mT for experimental longitudinal relaxation rates. The standard deviations of the values are about 30%. The measured values of phase relaxation rate are significantly higher than the low-field limit for the values of $(T_1)^{-1}$ and are almost independent of magnetic field strength. The upper solid curve corresponds to transverse phase relaxation time and was calculated with the same parameters τ and Δ using eqn. (8) where in the right-hand part a field-independent contribution from $(T_2^*)^{-1} = 0.016$ ns⁻¹ was added.

Thus, two relaxation mechanisms are required for a satisfactory description of the observed dependence of relaxation rates on the magnetic field strength. The first one corresponds to the Redfield theory, and the second one contributes only to phase relaxation.

The first mechanism is likely to be related to hfc modulation due to the rotations of methyl groups. For the (HME)⁺ radical cation recorded in a Freon matrix at 55 K, hfc with six equivalent protons and the constant $a(6H) = 2.75$ mT has been observed. Being heated to 140 K, this hfc is replaced by hfc with 18 protons and the constant $a(18H) = 1.22$ mT.¹⁸ As follows, the value $a(6H)$ that determines the perturbation amplitude during the fast rotation of methyl groups is close to our Δ value. For the Arrhenius dependence of rotation frequency on temperature the correlation time $\tau = 10$ ps, corresponds to the

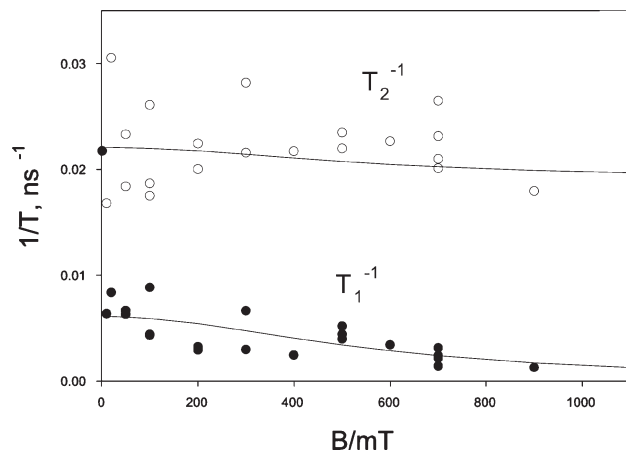


Fig. 6 Dependence of the reverse relaxation times T_1 and T_2 on magnetic field strength. Solid lines—calculation in the framework of the model of two relaxation mechanisms (see the text).

preexponent value of 10^{13} and the activation energy of 2.8 kcal/mole. The values are in agreement with literature data.²⁴

The second, magnetic field-independent contribution to T_2 relaxation has a number of possible causes. Its origin can be assumed to be an interaction between a radical ion and paramagnetic particles in a radiation track, which can be the exchange, and dipole-dipole interaction with neutral radicals or the triplet excited molecules forming in the track. Another explanation of this mechanism nature can be reversible charge transfer between radical ions and some impurities, presenting in the irradiated solution.²⁵

Apart from true phase relaxation, there are also inhomogeneous broadening of spectral lines and some instrumental effects that could cause a dephasing of spin evolution.

Numerical simulation has demonstrated that taking into consideration a number of simple factors simulating phase relaxation cannot provide a quantitative agreement with experiment. Among those factors, the accuracy of the zero field setting ± 0.05 mT, an additional inhomogeneous broadening of the radical anion's line due to a small fraction of protons and ^{13}C nuclei in pTP- d_{14} , a possible inhomogeneous broadening of the EPR spectrum of (HME)⁺ radical cation due to interaction with solvent molecules or formation of weakly bound dimers have been analyzed.

The short phase relaxation time can also be simulated by a transfer of the positive charge from HME radical cation to a solvent impurity molecule. If, for example, in such transfer the forming impurity radical cation has a $h\nu$ greater than that in HME radical cation, then the effective relaxation rate will be close to the charge transfer rate. Special experiments have shown that this mechanism is not likely to account for the contribution to the phase relaxation rate. To this end, we studied the effect of cyclic alkane *trans*-decalin and olefin cyclohexene solutes on the TR MFE curves. It was found that *trans*-decalin in concentrations up to 10^{-2} M does not affect the pattern of the TR MFE curve, while 10^{-2} M cyclohexene shortens the phase relaxation time down to 20 ns.

According to the results of chromatographic analysis, the major impurities (10^{-2} M by order of magnitude) in the solvent *n*-hexane that we used are its isomers branched alkanes, while the concentration of olefin impurities is 10^{-4} by order of magnitude. *trans*-Decalin has a lower ionization potential (9.32 ± 0.05 eV)²⁶ than *n*-hexane's isomers (from 9.8 to 10 eV).²⁷ Cyclohexene has a lower ionization potential (8.95 ± 0.01 eV)²⁰ than hexene-1 (9.44 ± 0.04 eV).²⁰ It is known that the effectiveness of the charge transfer correlates with the difference in ionization potentials of the molecules involved. Therefore one can expect that HME radical cation would deliver positive charge to alkane impurities less effectively than to *trans*-decalin, and to olefin impurities less effectively than to cyclohexene. This suggests that such mechanism cannot cause additional phase relaxation with a time shorter than 2000 ns.

Thus, in our view the most probable causes of the magnetic field-independent contribution to phase relaxation are interactions of radical ions with paramagnetic species in radiation track. Further progress in understanding those processes requires extra studies to be performed.

Conclusions

The hexamethylethane radical cation is used to demonstrate that the values of the EPR spectrum parameters of radical ions composing the spin-correlated radical pairs can be reliably determined from the TR MFE data. Recording by the OD EPR method requires mw field of large amplitude, which leads to the additional broadening of spectral lines. Thus, the characteristics such as the values of relaxation times can be determined by the TR MFE method more accurately. Moreover, it is possible to study their dependencies on the magnetic field

strength. This opens up new opportunities for studying the mechanisms of paramagnetic relaxation.

Acknowledgements

The work was supported by RFBR (grant 02-03-32224), INTAS (grant 00-0093), grant 'Support of leading scientific schools' No 84.2003.3 and the Russian Universities program (grant UR.05.01.023).

References

- 1 K. Nunome, K. Toriyama and M. Iwasaki, *J. Chem. Phys.*, 1983, **79**, 2499–2503.
- 2 R. Mehnert, in *Radical Ionic Systems*, ed. A. Lund and M. Shiotani, Kluwer Academic Publishers, Dordrecht, The Netherlands, 1991, pp. 231–284.
- 3 J. M. Warman, in *The Study of Fast Processes and Transient Species by Electron Pulse Radiolysis*, ed. J. H. Baxendale and F. Busi, D. Reidel, Dordrecht, 1982, pp. 433–533.
- 4 I. A. Shkrob, M. C. Sauer and A. D. Trifunac, in *Radiation Chemistry. Present Studies and Future Trends*, Elsevier, Amsterdam, 2001, pp. 175–221.
- 5 O. A. Anisimov, in *Radical Ionic Systems*, ed. A. Lund and M. Shiotani, Kluwer Academic Publishers, Dordrecht, The Netherlands, 1991, pp. 285–309.
- 6 A. D. Trifunac and D. W. Werst, in *Radical Ionic Systems*, ed. A. Lund and M. Shiotani, Kluwer Academic Publishers, Dordrecht, The Netherlands, 1991, pp.195–230.
- 7 A. V. Veselov, V. I. Melekhov, O. A. Anisimov and Yu. N. Molin, *Chem. Phys. Lett.*, 1987, **136**, 263–266.
- 8 B. Brocklehurst, *J. Chem. Soc. Faraday Trans.*, 1997, **93**, 1079–1087.
- 9 V. A. Bagryansky, O. M. Usov, V. I. Borovkov, T. V. Kobzeva and Yu. N. Molin, *Chem. Phys.*, 2000, **255**, 237–245.
- 10 V. I. Borovkov, V. A. Bagryansky, I. V. Eletsikh and Yu. N. Molin, *Mol. Phys.*, 2002, **100**, 1379–1384.
- 11 V. I. Borovkov, V. A. Bagryansky, Yu. N. Molin, M. P. Egorov and O. M. Nefedov, *Phys. Chem. Chem. Phys.*, 2003, **5**, 2027–2033.
- 12 K. M. Salikhov, Yu. N. Molin, R. Z. Sagdeev and A. L. Buchachenko, *Spin Polarization and Magnetic Effects in Chemical Reactions*, Elsevier, Amsterdam, 1984, p. 419.
- 13 V. O. Saik, N. N. Lukzen, V. M. Grigoryants, O. A. Anisimov, A. B. Doktorov and Yu. N. Molin, *Chem. Phys.*, 1984, **84**, 421.
- 14 K. Schulten and P. G. Wolynes, *J. Chem. Phys.*, 1978, **68**, 3292.
- 15 S. V. Anishchik, V. M. Grigoryantz, I. V. Shebolaev, Yu. D. Chernousov, O. A. Anisimov and Yu. N. Molin, *Pr. Tekhn. Eksp.*, 1989, **4**, 74–76.
- 16 V. I. Borovkov, S. V. Anishchik and O. A. Anisimov, *Chem. Phys. Lett.*, 1997, **270**, 327–332.
- 17 O. A. Anisimov, V. M. Grigoryantz, V. I. Melekhov, V. I. Korsunskij and Yu. N. Molin, *Dokl. Akad. Nauk SSSR*, 1981, **260**, 1151–1153.
- 18 D. W. Werst, M. G. Bakker and A. D. Trifunac, *J. Am. Chem. Soc.*, 1990, **112**, 40–50.
- 19 D. W. Werst, M. G. Bakker and A. D. Trifunac, *J. Phys. Chem.*, 1991, **95**, 3466–3477.
- 20 S. G. Lias, in *NIST Chemistry WebBook, NIST Standard Reference Database Number 69*, ed. P. J. Linstrom and W. G. Mallard, National Institute of Standards and Technology, Gaithersburg MD, March 2003, 20 899 (<http://webbook.nist.gov>).
- 21 T. Shida, H. Kubodera and Y. Egava, *Chem. Phys. Lett.*, 1981, **79**, 179–182.
- 22 V. M. Grigoryants, B. M. Tadjikov, O. M. Usov and Yu. N. Molin, *Chem. Phys. Lett.*, 1995, **246**, 392.
- 23 C. P. Slichter, *Principles of Magnetic Resonance*, Springer, Berlin, 1996.
- 24 J. R. Harbrige, S. S. Eaton and G. R. Eaton, *J. Phys. Chem.*, 2003, **107**, 598–609.
- 25 I. A. Shkrob, A. D. Liu, M. C. Sauer and A. D. Trifunac, *J. Phys. Chem.*, 2001, **105**, 7211–7215.
- 26 A. I. Mikaya and V. G. Zaikin, *Izv. Akad. Nauk SSSR, Ser. Khim.*, 1980, **6**, 1286.
- 27 NIST Standard Reference Database Number 69-March, 2003 Release <http://webbook.nist.gov/>.